

Structural Basis for the Potent and Selective Inhibition of Casein Kinase 1 Epsilon

Alexander M. Long,^{†,§} Huilin Zhao,^{‡,§} and Xin Huang^{†,*}[†]Department of Molecular Structure and Characterization, [‡]Department of Protein Technology, Amgen Inc., 360 Binney Street, Cambridge, Massachusetts 02142, United States

Supporting Information

ABSTRACT: Casein kinase 1 epsilon (CK1 ϵ) and its closest homologue CK1 δ are key regulators of diverse cellular processes. We report two crystal structures of PF4800567, a potent and selective inhibitor of CK1 ϵ , bound to the kinase domains of human CK1 ϵ and CK1 δ as well as one apo CK1 ϵ crystal structure. These structures provide a molecular basis for the strong and specific inhibitor interactions with CK1 ϵ and suggest clues for further development of CK1 δ inhibitors.

INTRODUCTION

The casein kinase 1 (CK1) family of highly conserved serine/threonine protein kinases has six human isoforms α , $\gamma 1$, $\gamma 2$, $\gamma 3$, δ , and ϵ that are involved in the regulation of diverse cellular processes including Wnt signaling, circadian rhythms, cellular signaling, membrane trafficking, cytoskeleton maintenance, DNA replication, DNA damage, and RNA metabolism.¹ CK1 δ and CK1 ϵ (CK1 δ/ϵ), two closely related CK1 isoforms, have recently gained increased attention as potential drug targets. CK1 δ/ϵ phosphorylate certain clock-related proteins as part of a complex arrangement of transcriptional/translational feedback loops that compromise the circadian oscillator in mammals.² CK1 δ/ϵ are also two key mediators of the Wnt signaling pathway, and several studies have highlighted their roles in cell survival and cancer progression.³ Moreover, both CK1 δ/ϵ were suggested to be involved in psychostimulant-induced behaviors by acting on the Darpp-32-PP1 signaling pathway to regulate AMPA receptor phosphorylation in the nucleus accumbens.⁴ Thus, inhibition of the kinase activity of CK1 δ/ϵ is a promising strategy for multiple therapies in the treatment of abnormal circadian behavior, cancer, and drug use disorders.

PF670462 (**1**, Figure 1A), a novel and potent small molecule pan-CK1 δ/ϵ inhibitor (IC₅₀ = 13–80 nM) with good selectivity over other kinases,⁵ was shown to alter CK1 δ/ϵ dependent processes in circadian rhythms in both cultured cells and in animals.⁶ Intriguingly, **1** significantly reduces the growth rate of ovarian cancer cells independent of the wnt/ β -catenin pathway⁷ but only modestly inhibits the proliferation of some other cancer cells despite being a potent inhibitor of Wnt signaling.⁸ **1** also blocks methamphetamine/amphetamine induced locomotion and decreases Darpp-32 phosphorylation in mice.⁴ These results suggest that CK1 δ/ϵ are important in the regulation of circadian clock, ovarian cancer growth/survival, and sensitivity to drug abuse. However, it remains unclear whether one of the CK1 δ/ϵ kinases has a predominant role because PF670462 is very potent for both CK1 δ (IC₅₀ = 13 nM) and CK1 ϵ (IC₅₀ = 80 nM). A potent and selective small-molecule inhibitor of CK1 ϵ has been recently reported and has proved useful in probing unique roles between CK1 δ

and CK1 ϵ . PF4800567 (**2**, Figure 1A) had an IC₅₀ of 32 nM for CK1 ϵ and displayed greater than 22-fold selectivity over CK1 δ (IC₅₀ = 711 nM) and even greater selectivity against other kinases.^{5b} While **1** causes a significant phase delay in animal models of circadian rhythm, **2** has only a minimal effect on the circadian clock at concentrations substantially over its CK1 ϵ IC₅₀, indicating that CK1 ϵ is not the predominant mediator of circadian timing compared to CK1 δ .^{5b,9} **2** has a similar growth inhibition effect on ovarian cancer cells as **1**, demonstrating the likely importance of CK1 ϵ in regulating their proliferation, which is also confirmed by shRNA knockdown of CK1 ϵ .⁷ Both **2** and CK1 ϵ knockout increase the locomotor stimulant response to methamphetamine whereas **1** has the opposite effect, suggesting that CK1 ϵ and CK1 δ are negative and positive regulators respectively of sensitivity to psychostimulants.¹⁰

Crystal structures of CK1 δ in the apo form and in complex with **1** revealed that the side chain of the gatekeeper residue Met82 is rotated toward Pro66 in the complex structure to avoid a steric clash with **1** and engages in strong hydrophobic interactions with **1** instead.¹¹ The side chain rotation of Met82 is only possible due to the small side chain of Pro66, and only a few kinases (such as CK1 ϵ) have residues with small side chain at the position equivalent to Pro66 in CK1 δ , resulting in the high selectivity of **1** over other kinases. However, no crystal structure of CK1 ϵ has been reported, and it is not obvious from the CK1 δ crystal structures why **2** is more than 22-fold more selective for CK1 ϵ over CK1 δ despite identical ATP binding site and >98% sequence identity between these two kinases (Figure 1B). Herein, we report the crystal structures of human CK1 δ and CK1 ϵ in complex with **2** as well as apo CK1 ϵ and describe the structural basis for the inhibitor's potency and selectivity for CK1 ϵ over CK1 δ and other kinases, which are further validated by mutagenesis analysis.

Received: September 18, 2012

Published: October 29, 2012

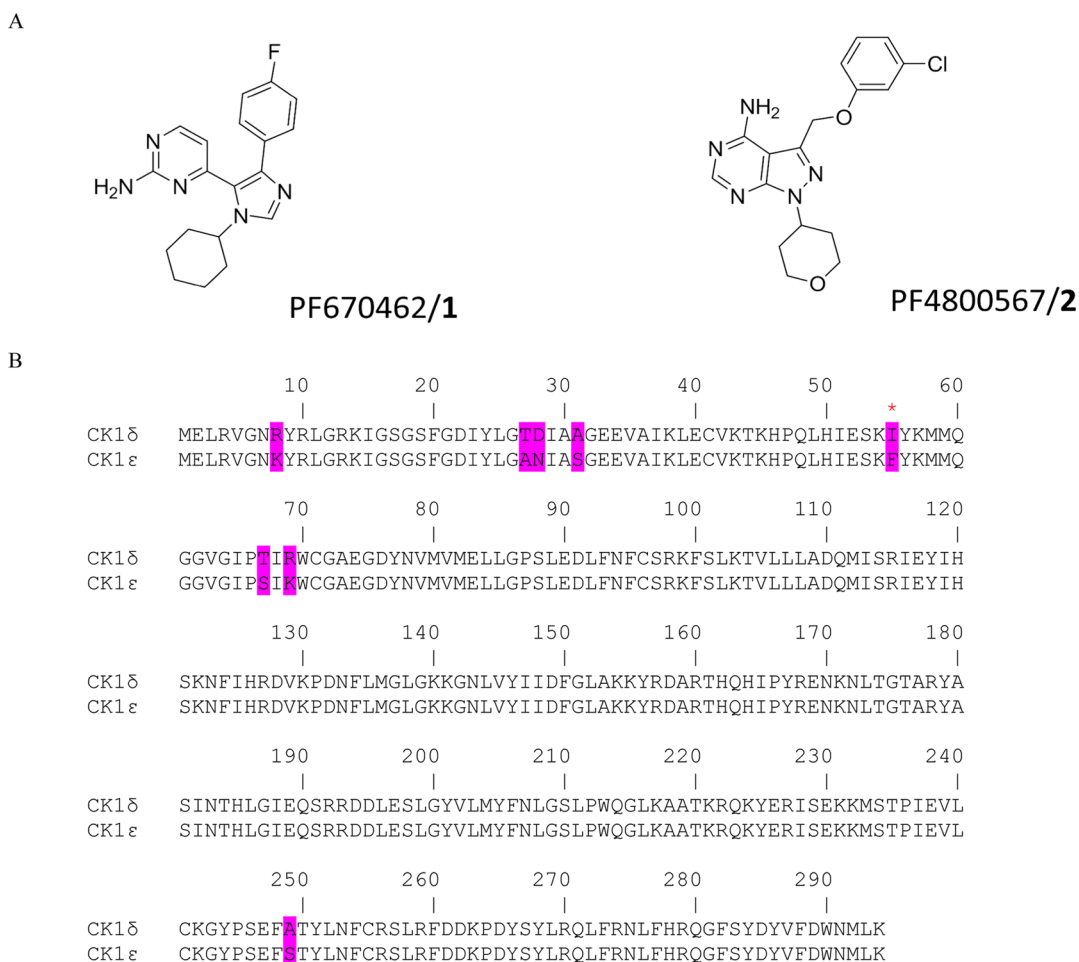


Figure 1. (A) Molecular structure of **1** and **2**. (B) Sequence alignment of CK1 δ and CK1 ϵ and kinase domains, with nonidentical residues highlighted.

RESULTS AND DISCUSSION

Co-crystallization of dephosphorylated CK1 δ kinase domain with **2** yielded crystals that diffracted to 2.07 Å resolution. The two CK1 δ /2 complexes observed in this crystal structure are highly similar (with a backbone rmsd of 0.8 Å). The CK1 δ /2 complex structure (Figure 2A) reveals that **2** is anchored in the ATP binding site of CK1 δ by interactions similar to those observed in CK1 δ /1 complexes. The amino pyrimidine group of **2** forms two hydrogen bonds with the carbonyl oxygen of Glu83 and the main chain NH of Leu85 from the interlobe linker (hinge) polypeptide of CK1 δ . The *meta*-chlorophenyl moiety of **2** is buried deeply in CK1 δ , forming strong hydrophobic interactions with the side chains of Met80 and Met82. The side chain of Met82 is rotated toward Pro66. The interactions of the *meta* chlorophenyl group of **2** with residues Met82 and Pro66 of CK1 δ , similar to those of the *para* fluorophenyl of **1**, likely account for the high selectivity of **2** over other kinases. However, the structure also shows that the eight residues (amino acid 8, 27, 28, 31, 55, 67, 69, and 249) that are different between CK1 δ and CK1 ϵ in the kinase domain are more than 9 Å from **2**, making it difficult to explain the >22-fold selectivity of **2** for CK1 ϵ over CK1 δ .

To better understand this selectivity of **2**, we determined the crystal structure of CK1 ϵ kinase domain in complex with **2** at 2.74 Å resolution (Figure 2B). Dephosphorylated CK1 ϵ (1–294) complexed with **2** was cocrystallized in a crystal form that

is different from that of CK1 δ (1–294) complexed with **2**. The two CK1 ϵ /2 complexes observed in this crystal structure are highly similar. Reminiscent of the CK1 δ /2 structure, the amino pyrimidine group of **2** forms two hydrogen bonds with the interlobe linker of CK1 ϵ and the *meta*-chlorophenyl moiety of **2** is buried deeply in CK1 ϵ , forming strong hydrophobic interactions with the side chains of Met80 and Met82. The side chain of Met82 is also rotated toward Pro66 in the CK1 ϵ /2 structure. Strikingly, structural comparison of the CK1 ϵ /2 and the CK1 δ /2 complexes reveals one obvious difference: the DFG motif of CK1 ϵ in the CK1 ϵ /2 complex is flipped by ~180° compared to the DFG motif of CK1 δ in the CK1 δ /2 complex and is involved in additional strong hydrophobic interaction with the *meta*-chlorophenyl group. This provides an explanation for why **2** is a much more potent inhibitor for CK1 ϵ than CK1 δ . On the other hand, structural superposition of the CK1 ϵ /2 and the CK1 δ /1 complexes suggests that the side chain of the Phe150 of the “flipped” DFG motif in CK1 ϵ would clash with the imidazole of **1**, and it is likely that the DFG motif of CK1 δ adopts the same conformation as that of CK1 ϵ when **1** is bound. This is consistent with **1** being an equally potent inhibitor of CK1 ϵ and CK1 δ .

This unique conformation of the DFG motif of CK1 ϵ adopted in the CK1 ϵ /2 structure was also not observed in the unliganded CK1 ϵ structure determined at 2.77 Å resolution (Figure 2C). The 12 CK1 ϵ molecules observed in this apo crystal structure are very similar to each other, and all the DFG

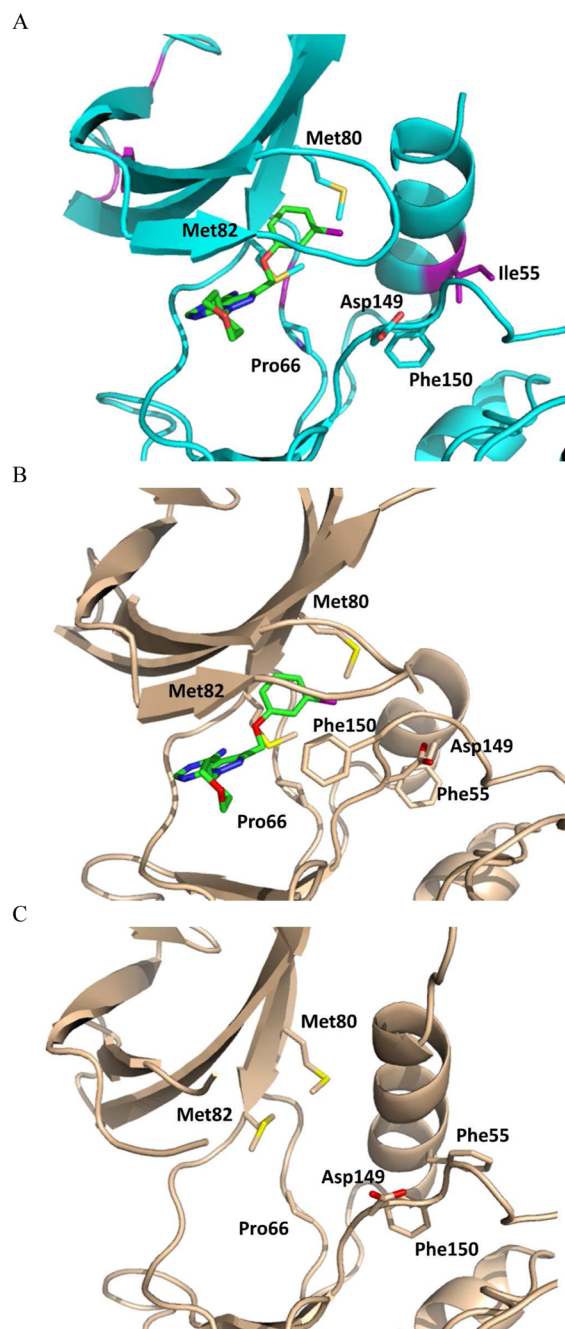


Figure 2. (A) The ATP binding site, showing interactions between **2** and CK1 δ residues. For **2**, carbon, nitrogen, and chlorine atoms are shown in green, blue, and purple, respectively. Residues that are different from CK1 ϵ are colored in purple. The DFG motif adopts a “DFG-in” conformation. (B) The ATP binding site, showing interactions between **2** and CK1 ϵ residues. The DFG motif adopts a “DFG-out” conformation. (C) The ATP binding site of apo CK1 ϵ . The DFG motif adopts a “DFG-in” conformation.

motifs adopt a “DFG-in” conformation where the side chain of Phe150 of the DFG motif is buried in a deep hydrophobic pocket formed by the side chains of Tyr56, Met59, Ile115, Ile119, His126, and Ile147. The same “DFG-in” conformation has been adopted by the DFG motif of CK1 δ in both apo and complex structures. In comparison, the DFG motif in the CK1 ϵ /**2** complex adopts a “DFG-out” conformation where the Phe150 is flipped out of this hydrophobic pocket to be involved in hydrophobic interactions with the inhibitor and the side

chain of Phe55 from the α C helix is rotated into the hydrophobic pocket to maintain similar hydrophobic interactions. The DFG motif and the hydrophobic pocket are completely conserved between CK1 ϵ and CK1 δ , but Phe55 of CK1 ϵ is replaced by Ile55 in CK1 δ , which could not engage in the same strong interactions with the hydrophobic pocket to stabilize the “DFG-out” conformation of the DFG motif, resulting in much weaker inhibition of CK1 δ by **2**.

To evaluate the importance of residue 55 in the inhibition of **2** between CK1 ϵ and CK1 δ , we mutated Phe55 to Ile55 in CK1 ϵ and Ile55 to Phe55 in CK1 δ and then carried out a differential scanning fluorimetry (DSF) binding assay to monitor whether these mutations altered the interactions with **2** (Table 1). DSF measures the shifts of melting

Table 1. Differential Scanning Fluorimetry (DSF) Binding Studies of **1** and **2** to Wild-Type and Mutant CK1 δ / ϵ

ΔT_m ($^{\circ}$ C)		1	2
CK1 δ	wild-type	9.6 \pm 0.1	4.8 \pm 0.1
	I55F	9.6 \pm 0.1	13.2 \pm 0.1
	T67S	9.6 \pm 0.1	4.8 \pm 0.1
	R69K	9.6 \pm 0.1	4.8 \pm 0.1
CK1 ϵ	wild-type	8.6 \pm 0.1	11.5 \pm 0.1
	F55I	10.4 \pm 0.1	6.4 \pm 0.1
	S67T	8.6 \pm 0.1	11.5 \pm 0.1
	K69R	8.6 \pm 0.1	11.5 \pm 0.1

temperature (T_m) of proteins in the presence of compounds, and it has been previously used for rapid chemical profiling of protein kinases.¹² Wild-type CK1 δ was stabilized significantly by **1** ($\Delta T_m = 9.6$ $^{\circ}$ C) but less so by **2** ($\Delta T_m = 4.8$ $^{\circ}$ C), in good agreement with the enzymatic data that **1** ($IC_{50} = 13$ nM) inhibits CK1 δ much more strongly than **2** ($IC_{50} = 711$ nM).^{5b} Wild-type CK1 ϵ was stabilized significantly by **1** ($\Delta T_m = 8.6$ $^{\circ}$ C) and even more by **2** ($\Delta T_m = 11.5$ $^{\circ}$ C), consistent with the enzymatic data that **2** ($IC_{50} = 32$ nM) is an even more potent inhibitor than **1** ($IC_{50} = 80$ nM) for CK1 ϵ .^{5b} In sharp contrast, the T_m of CK1 ϵ Ile55Phe was shifted by 9.6 $^{\circ}$ C in the presence of **1** and by 13.2 $^{\circ}$ C in the presence of **2**, similar to the wild-type CK1 ϵ , while the T_m of CK1 δ Phe55Ile was shifted by 10.4 $^{\circ}$ C in the presence of **1** and by only 6.4 $^{\circ}$ C in the presence of **2**, reminiscent of the wild-type CK1 δ . In comparison, mutations of other nonconserved residues such as 67 and 69 of CK1 ϵ and CK1 δ , which are slightly closer to the inhibitors than residue 55, did not change the stabilization profile at all. These results further support that the difference of residue 55 between CK1 ϵ and CK1 δ accounts for the selectivity of **2** for CK1 ϵ over CK1 δ . Phe55 is also not conserved in other kinases, and it is not surprising that **2** displayed much greater selectivity for CK1 ϵ over other kinases than **1**.

Our CK1 ϵ /**2** complex structure also suggests routes to further optimize CK1 ϵ inhibitors. As mentioned above, the *meta*-chlorophenyl is involved in hydrophobic interaction with the side chain of Phe150 of the “flipped” DFG motif of CK1 ϵ . It appears that ortho substitutions such as fluoro or methyl at position 2 of the *meta*-chlorophenyl could form an additional hydrophobic interaction with the side chain of Phe150, resulting in a potential improvement in potency and selectivity.

In summary, the present structural and mutagenesis studies provide insights into the molecular basis for the interactions of **2** with CK1 ϵ , which will be important for further optimization of CK1 ϵ inhibitors.

EXPERIMENTAL SECTION

Human CK1 δ (1–294) was expressed and purified as previously described.¹¹ Human CK1 ϵ (1–294) was expressed and purified similarly to human CK1 δ (1–294), except that the expression was carried out in Rosetta(DE3). **2** (>99% purity by HPLC) was purchased from Tocris Bioscience, and crystals of CK1 δ complexed with **2** were obtained in hanging drops with 100 mM citrate pH 5.0, 1.0 M LiCl, 20–30% PEG6000. These crystals belong to the space group C2 with unit cell parameters of $a = 171.22$, $b = 48.10$, $c = 80.47$ Å, and $\beta = 110.67^\circ$. Crystals of CK1 ϵ /2 were obtained in hanging drops with 100 mM Hepes pH 7.5, 3% ethanol, and 1.1–1.6 M (NH₄)₂SO₄. These crystals belong to the space group P4₃2₁2, with unit cell parameters of $a = b = 111.11$ and $c = 155.43$ Å. Crystals of CK1 ϵ were obtained in hanging drops with 100 mM Hepes pH 7.5, and 1.0–1.5 M (NH₄)₂SO₄. These crystals belong to the space group C2 with unit cell parameters of $a = 180.36$, $b = 142.50$, $c = 232.46$ Å, and $\beta = 73.86^\circ$. Paratone-N mineral oil was used as cryoprotectant. Diffraction data for all crystals in this work were collected on beamline 21-ID-F at the Advanced Photon Source (APS) and processed and scaled with HKL 2000. All three structures were solved by molecular replacement with PHASER using our CK1 δ /1 (PDB code 3UZP) structure as the template. Model building was carried out with QUANTA, and refinement was done using CNS. Details on data processing and refinement statistics are given in the Supporting Information, Table S1. $2f_o - f_c$ electron density maps of the ATP binding sites before any ligand building are shown in Supporting Information, Figure S1.

CK1 δ mutants such as Ile55Phe and CK1 ϵ mutants such as Phe55Ile were expressed and purified as wild-type CK1 δ and CK1 ϵ , respectively. Proteins were diluted to 0.1 mg/mL in buffer containing 100 mM Hepes, pH 7.5, and 150 mM NaCl containing 1:1000 SyproOrange (Invitrogen). Then 25 μ L of protein solution were added to all wells in 96-well clear plates (Roche Diagnostics), each well containing 0.25 μ L 10 mM compound solution (thus 100 μ M final compound concentration) or 0.25 μ L pure DMSO as the references. The plates were spun at 1000 rpm and then sealed by tape (Roche Diagnostics). Thermal stability was measured by monitoring SyproOrange fluorescence ($\lambda_{\text{excitation}} = 465$ nm and $\lambda_{\text{emission}} = 580$ nm) while heating the samples from 20 to 90 °C in increments of 1 °C/min in a real-time PCR system LightCycler480 (Roche Diagnostics). Each experiment was carried out in triplicate.

ASSOCIATED CONTENT

Supporting Information

Details on data processing and refinement statistics. This material is available free of charge via the Internet at <http://pubs.acs.org>.

Accession Codes

Coordinates for the CK1 δ and **2**, CK1 ϵ and **2**, and CK1 ϵ structures have been deposited in the Protein Data Bank with access codes 4HNF, 4HNI, and 4HOK.

AUTHOR INFORMATION

Corresponding Author

*Phone: 617-444-5045; Fax: 617-577-9511. E-mail: hxin@amgen.com).

Author Contributions

[§]These authors contributed equally to this work

Notes

The authors declare no competing financial interest.

ACKNOWLEDGMENTS

We are grateful to Drs. Paul Rose, Doug Whittington, and Nigel Walker for critical review of the manuscript.

ABBREVIATIONS USED

CK1, casein kinase 1; T_m , melting temperature; ΔT_m , shift in melting temperature

REFERENCES

- (1) (a) Vielhaber, E.; Virshup, D. M. Casein kinase I: from obscurity to center stage. *IUBMB Life* **2001**, *51* (2), 73–78. (b) Knippschild, U.; Gocht, A.; Wolff, S.; Huber, N.; Lohler, J.; Stoter, M. The casein kinase I family: participation in multiple cellular processes in eukaryotes. *Cell Signalling* **2005**, *17* (6), 675–689. (c) Price, M. A. CK1, there's more than one: casein kinase I family members in Wnt and Hedgehog signaling. *Genes Dev.* **2006**, *20* (4), 399–410. (d) Virshup, D. M.; Eide, E. J.; Forger, D. B.; Gallego, M.; Harnish, E. V. Reversible protein phosphorylation regulates circadian rhythms. *Cold Spring Harbor Symp. Quantum Biol.* **2007**, *72*, 413–420.
- (2) (a) Eide, E. J.; Vielhaber, E. L.; Hinz, W. A.; Virshup, D. M. The circadian regulatory proteins BMAL1 and cryptochromes are substrates of casein kinase Iepsilon. *J. Biol. Chem.* **2002**, *277* (19), 17248–17254. (b) Eide, E. J.; Woolf, M. F.; Kang, H.; Woolf, P.; Hurst, W.; Camacho, F.; Vielhaber, E. L.; Giovanni, A.; Virshup, D. M. Control of mammalian circadian rhythm by CKIepsilon-regulated proteasome-mediated PER2 degradation. *Mol. Cell. Biol.* **2005**, *25* (7), 2795–2807. (c) Xu, Y.; Padiath, Q. S.; Shapiro, R. E.; Jones, C. R.; Wu, S. C.; Saigoh, N.; Saigoh, K.; Ptacek, L. J.; Fu, Y. H. Functional consequences of a CKIdelta mutation causing familial advanced sleep phase syndrome. *Nature* **2005**, *434* (7033), 640–644.
- (3) (a) Grueneberg, D. A.; Degot, S.; Pearlberg, J.; Li, W.; Davies, J. E.; Baldwin, A.; Endege, W.; Doench, J.; Sawyer, J.; Hu, Y.; Boyce, F.; Xian, J.; Munger, K.; Harlow, E. Kinase requirements in human cells: I. Comparing kinase requirements across various cell types. *Proc. Natl. Acad. Sci. U. S. A.* **2008**, *105* (43), 16472–16477. (b) Yang, W. S.; Stockwell, B. R. Inhibition of casein kinase I-epsilon induces cancer-cell-selective, PERIOD2-dependent growth arrest. *Genome Biol.* **2008**, *9* (6), R92. (c) Brockschmidt, C.; Hirner, H.; Huber, N.; Eismann, T.; Hillenbrand, A.; Giamas, G.; Radunsky, B.; Ammerpohl, O.; Bohm, B.; Henne-Bruns, D.; Kalthoff, H.; Leithauser, F.; Trauzold, A.; Knippschild, U. Anti-apoptotic and growth-stimulatory functions of CK1 delta and epsilon in ductal adenocarcinoma of the pancreas are inhibited by IC261 in vitro and in vivo. *Gut* **2008**, *57* (6), 799–806.
- (4) Li, D.; Herrera, S.; Bubula, N.; Nikitina, E.; Palmer, A. A.; Hancock, D. A.; Loweth, J. A.; Vezina, P. Casein kinase I enables nucleus accumbens amphetamine-induced locomotion by regulating AMPA receptor phosphorylation. *J. Neurochem.* **2011**, *118* (2), 237–247.
- (5) (a) Badura, L.; Swanson, T.; Adamowicz, W.; Adams, J.; Cianfrogna, J.; Fisher, K.; Holland, J.; Kleiman, R.; Nelson, F.; Reynolds, L.; St. Germain, K.; Schaeffer, E.; Tate, B.; Sprouse, J. An inhibitor of casein kinase I epsilon induces phase delays in circadian rhythms under free-running and entrained conditions. *J. Pharmacol. Exp. Ther.* **2007**, *322* (2), 730–738. (b) Walton, K. M.; Fisher, K.; Rubitski, D.; Marconi, M.; Meng, Q. J.; Sladek, M.; Adams, J.; Bass, M.; Chandrasekaran, R.; Butler, T.; Griffor, M.; Rajamohan, F.; Serpa, M.; Chen, Y.; Claffey, M.; Hastings, M.; Loudon, A.; Maywood, E.; Ohren, J.; Doran, A.; Wager, T. T. Selective inhibition of casein kinase I epsilon minimally alters circadian clock period. *J. Pharmacol. Exp. Ther.* **2009**, *330* (2), 430–439.
- (6) Sprouse, J.; Reynolds, L.; Kleiman, R.; Tate, B.; Swanson, T. A.; Pickard, G. E. Chronic treatment with a selective inhibitor of casein kinase I delta/epsilon yields cumulative phase delays in circadian rhythms. *Psychopharmacology (Berlin)* **2010**, *210* (4), S69–S76.
- (7) Rodriguez, N.; Yang, J.; Hasselblatt, K.; Liu, S.; Zhou, Y.; Rauh-Hain, J. A.; Ng, S. K.; Choi, P. W.; Fong, W. P.; Agar, N. Y.; Welch, W. R.; Berkowitz, R. S.; Ng, S. W. Casein kinase I epsilon interacts with mitochondrial proteins for the growth and survival of human ovarian cancer cells. *EMBO Mol. Med.* **2012**, DOI: 10.1002/emmm.201101094.
- (8) Cheong, J. K.; Nguyen, T. H.; Wang, H.; Tan, P.; Voorhoeve, P. M.; Lee, S. H.; Virshup, D. M. IC261 induces cell cycle arrest and apoptosis of human cancer cells via CK1delta/varepsilon and Wnt/

beta-catenin independent inhibition of mitotic spindle formation. *Oncogene* **2011**, *30* (22), 2558–2569.

(9) Meng, Q. J.; Maywood, E. S.; Bechtold, D. A.; Lu, W. Q.; Li, J.; Gibbs, J. E.; Dupre, S. M.; Chesham, J. E.; Rajamohan, F.; Knafels, J.; Sneed, B.; Zawadzke, L. E.; Ohren, J. F.; Walton, K. M.; Wager, T. T.; Hastings, M. H.; Loudon, A. S. Entrainment of disrupted circadian behavior through inhibition of casein kinase 1 (CK1) enzymes. *Proc. Natl. Acad. Sci. U. S. A.* **2010**, *107* (34), 15240–15245.

(10) Bryant, C. D.; Parker, C. C.; Zhou, L.; Olker, C.; Chandrasekaran, R. Y.; Wager, T. T.; Bolivar, V. J.; Loudon, A. S.; Vitaterna, M. H.; Turek, F. W.; Palmer, A. A. Csnk1e is a genetic regulator of sensitivity to psychostimulants and opioids. *Neuro-psychopharmacology* **2012**, *37* (4), 1026–1035.

(11) Long, A.; Zhao, H.; Huang, X. Structural basis for the interaction between casein kinase 1 delta and a potent and selective inhibitor. *J. Med. Chem.* **2012**, *55* (2), 956–960.

(12) (a) Vedadi, M.; Niesen, F. H.; Allali-Hassani, A.; Fedorov, O. Y.; Finerty, P. J., Jr.; Wasney, G. A.; Yeung, R.; Arrowsmith, C.; Ball, L. J.; Berglund, H.; Hui, R.; Marsden, B. D.; Nordlund, P.; Sundstrom, M.; Weigelt, J.; Edwards, A. M. Chemical screening methods to identify ligands that promote protein stability, protein crystallization, and structure determination. *Proc. Natl. Acad. Sci. U. S. A.* **2006**, *103* (43), 15835–15840. (b) Niesen, F. H.; Berglund, H.; Vedadi, M. The use of differential scanning fluorimetry to detect ligand interactions that promote protein stability. *Nature Protoc.* **2007**, *2* (9), 2212–2221. (c) Fedorov, O.; Marsden, B.; Pogacic, V.; Rellos, P.; Muller, S.; Bullock, A. N.; Schwaller, J.; Sundstrom, M.; Knapp, S. A systematic interaction map of validated kinase inhibitors with Ser/Thr kinases. *Proc. Natl. Acad. Sci. U. S. A.* **2007**, *104* (51), 20523–20528.